METEOSAT Observations of Longwave Cloud-Radiative Forcing for April 1985

JOHANNES SCHMETZ, MOHAMED MHITA AND LEO VAN DE BERG

European Space Agency (ESA), European Space Operations Centre (ESOC), Darmstadt, Federal Republic of Germany

(Manuscript received 15 August 1989, in final form 23 January 1990)

ABSTRACT

Outgoing longwave radiative fluxes (OLR) and the longwave cloud-radiative forcing at the top of the atmosphere are retrieved from METEOSAT radiance observations in the thermal infrared window (IR: 10.5–12.5 μm) and water vapor (WV: 5.7–7.1 μm) channels for April 1985. The analysis exploits an operationally preprocessed radiance dataset that includes a scene identification of clear sky, low level, medium level and high level clouds. Monthly means of the OLR and the longwave cloud-radiative forcing are inferred for areas of about 200 km $\times$ 200 km. Extended regions with a forcing larger than 60 W m^{-2} are found within the intertropical convergence zone (ITCZ) over southern Sudan and around 5°S over Brazil and the adjacent Atlantic Ocean.

The contribution of three levels of cloud to the longwave radiative forcing is estimated: high level clouds ($\leq$400 hPa) contribute about 80% to the total longwave forcing in regions with strong convective activity (ITCZ). Medium level clouds (700 $\leq$ cloud top $<$ 400 hPa) induce a maximum forcing of 15–20 W m^{-2} over the Ethiopian highland, while low level cloud forcing reaches values of 5–10 W m^{-2} over the marine stratocumulus regions and within the midlatitude westerlies.

Systematic errors in the longwave cloud-radiative forcing due to calibration errors, cloud contamination of clear sky radiances and a dry bias in the humidity of the upper troposphere, which may occur as a result of minimizing the cloud contamination, are discussed; it is concluded that the present study underestimates maximum values of the longwave cloud-radiative forcing by about 10 W m^{-2}.

1. Introduction

The role of clouds is one of the major uncertainties in the evaluation of the sensitivity of the earth's climate to perturbations. The effect of clouds on the outgoing longwave radiation field and the absorbed solar radiation is both potentially large and has opposing effects on the net radiation (Schneider 1972). The direct effect of clouds on net radiation is commonly termed "cloud forcing" (Coakley and Baldwin 1984; Charlock and Ramanathan 1985; Cess and Potter 1987; Hartmann et al. 1986; Ramanathan 1987); the longwave cloud radiative forcing may be written as

$$CF_{lw} = F_{cl} - F_a \tag{1}$$

or:

$$CF_{lw} = C(F_{cl} - F_{ov}), \tag{2}$$

where F_a is the area mean OLR, F_{cl} is the clear sky OLR, F_{ov} is the OLR for overcast sky, and C is the fractional cloud cover. In regions with multilayer clouds the contribution $CF_{lw,i}$ of an individual cloud layer i to the total forcing is

$$CF_{lw,i} = C_i(F_{cl} - F_{ov,i}), \tag{3}$$

where C_i is the fractional cloud cover by the layer i as observed from satellite and $F_{ov,i}$ is the OLR corresponding to that cloud scene. The total cloud forcing CF_{lw} equals the sum over the individual contribution terms $CF_{lw,i}$.

The concept of cloud-radiative forcing is appealing for its apparent simplicity as it does not require the explicit estimation of cloud parameters from satellite data: by estimating the total forcing CF_{lw} the problem reduces mainly to the retrieval of the clear sky fluxes F_{cl}. Observing and comprehending the cloud-radiative forcing is a first step toward understanding the cloud-radiative feedback to climate perturbations. Overviews of the topic are given by Ramanathan (1987) and Ramanathan et al. (1989); the latter paper also presents first results of the global shortwave and longwave components of the cloud forcing from ERBE (Earth Radiation Budget Experiment; Barkstrom and Smith 1986). The outstanding results of the analysis by Ramanathan et al. (1989) are first the global mean cloud forcing in the longwave and shortwave is about an order of magnitude larger than the radiative forcing from a CO_2 doubling, and second the net effect of the present cloud distribution appears to be a cooling of the earth.

This paper presents first results of the longwave cloud radiative forcing derived from METEOSAT. As the study is based on data from the present generation of geostationary satellites it suffers from shortcomings in calibration and the fact that observations of the radia-

Corresponding author address: Dr. Johannes Schmetz, European Space Observations Centre, European Space Agency, Robert-Bosch-Strasse 5, 6100 Darmstadt, West Germany.

tion budget at the top of the atmosphere have to be derived from narrow spectral intervals, although the use of the two METEOSAT channels in the thermal infrared (IR: 10.5–12.5 μm, WV: 5.7–7.1 μm) reduces the error in the OLR considerably (see Schmetz and Liu 1988; hereafter SL 1988). A strong side of geostationary is the good temporal sampling that is important to resolve the diurnal cycle (Harrison et al. 1989); in this study we use eight observations per day.

It is the primary purpose of this work to examine the feasibility of extracting longwave cloud-radiative forcing from METEOSAT radiance observations. A novel feature of the study is the differentiation between clouds at three altitude intervals, thus enabling an estimate of the vertical distribution of cloud forcing. The April 1985 period has been chosen since ERBE results from Ramanathan et al. (1989) are available for comparison. Similar results for July 1983 have been presented previously (Schmetz 1989a). Reasons for systematic differences between ERBE results and our study are discussed in detail in section 3.

2. Satellite data

The geostationary METEOSAT satellites observe the earth with an imaging radiometer in three channels: in the solar spectrum (VIS) between 0.4 and 1.1 μm, in the infrared window region (IR) between 10.5 and 12.5 μm and in the water vapor (WV) absorption band between 5.7 and 7.1 μm. Images are taken at half hourly intervals and the spatial sampling at the subsatellite point corresponds to 2.5 km $\times$ 2.5 km for the VIS, and 5 km $\times$ 5 km in the IR and WV channels.

a. The climatological dataset (CDS)

The present study uses preprocessed satellite data rather than the satellite raw radiance observations for individual pixels. The database is the "Climatological Data Set" (CDS), an operational product that is routinely derived and archived eight times per day (METEOSAT Exploitation Project 1987). Essentially the CDS is the output of a multispectral histogram analysis of simultaneous images taken in different channels. The aim of the multispectral image analysis (METEOSAT Exploitation Project 1987; Schmetz and Liu 1988) is to discriminate between the dominating scenes in segment areas of the satellite image; a segment corresponds to an area of 32 $\times$ 32 IR pixels or about 160 km $\times$ 160 km at nadir. The scenes can be sea, various types of land, and clouds at different altitudes.

The image analysis sequentially extracts clusters, corresponding to scenes, from multispectral histograms for a segment area. The identification of a cluster with a scene type, such as cloud, is aided by ancillary geographical data, and in particular, climatological radiances or the scene/radiance pair found in the previous analysis. Generally the scheme runs hourly and the use of the climatological information for aiding the scene identification is replaced by the previous results; this provides stable and consistent scene identifications since scene properties change slowly. A cluster of pixels pertaining to a scene is defined by its mean count, standard deviation, and the number of pixels.

The height attribution of clouds is based on the cluster mean brightness temperature and climatological temperature profiles or the temperature forecast profiles routinely received from the European Centre of Medium Range Weather Forecast (ECMWF). Forecast profiles are used for the height correction of semitransparent cloud with the method described by Bowen and Saunders (1984). A flag classifies clouds into three altitude intervals: low (>700 hPa), medium (700–400 hPa), and high cloud ($\leq$400 hPa).

The CDS is available eight times per day and allows the estimation of the contribution of various scenes to the OLR. The use of cluster mean radiances instead of pixel radiances does not lead to significant errors: SL (1988) found a mean difference between the OLR retrieved from high resolution data and from the CDS of less than 1 W m^{-2} and an rms error of the order of 4 W m^{-2}.

b. Radiance calibration

The CDS contains uncalibrated radiance data for the various scenes in terms of mean counts; therefore it is necessary to convert the count values to physical unit (radiances) before retrieving the OLR. The conversion of satellite observed counts Ct to radiances L follows a linear relationship for both the IR and WV channel:

$$L = \alpha(Ct - Ct_0) \quad (4)$$

where α is the calibration coefficient and Ct_0 the count at space view.

Calibration coefficients are routinely derived by vicarious methods using radiative transfer calculations; the present methods are described by Gaertner (1989) and Schmetz (1989b). It is important to mention that the WV calibration for the period under study followed a less rigorous approach that induced a low bias in the WV radiances; the matter will be discussed in more detail in section 3.

In the present study we use the following calibration coefficients taken from the quarterly calibration report (ESOC 1985): $\alpha_{IR} = 0.0490$ W m^{-2} sr^{-1} ct^{-1} and $\alpha_{WV} = 0.00785$ W m^{-2} sr^{-1} ct^{-1}; the space counts for the IR and WV channel are 5 and 6, respectively.

Note that the IR calibration does not require the "fine adjustment of gain" factor (Jones and Morgan 1981), as it would be applicable to raw counts, since the cluster mean counts have been adjusted accordingly.

c. OLR from IR and WV radiances

The OLR retrieval has been described in detail by SL (1988), basically it involves two steps:

(i) The filtered satellite radiances L_{ir} and L_{wv} are converted into unfiltered narrowband fluxes f_{ir} and f_{wv}; for instance the IR narrowband flux f_{ir} is obtained from

$$f_{ir} = a(\theta)L_{ir}(\theta) + b(\theta) \quad (5)$$

where θ is the satellite zenith angle and, following the formulation of Abel and Gruber (1979) for the limb darkening, the functions $a(\theta)$ and $b(\theta)$ can be written as

$$a(\theta) = k_1 + k_2(\sec\theta - 1) + k_3(\sec\theta - 1)^2 \quad (6)$$

$$b(\theta) = k_4 + k_5(\sec\theta - 1) + k_6(\sec\theta - 1)^2. \quad (7)$$

The coefficients k_i were determined from a regression analysis of results from a radiative transfer model.

(ii) The broadband outgoing longwave flux F is inferred from the narrowband fluxes f_{ir} and f_{wv} with a third-order polynomial:

$$F = \xi_0 + \sum_{i=1}^{3} \xi_i f_{ir}^i + \sum_{i=1}^{3} \zeta_i f_{wv}^i \quad (8)$$

where the coefficients ξ_i were again obtained from a regression analysis of model results. Both sets of coefficients k_i and ξ_i used in this work are taken from SL (1988).

Equation 8 can be used for estimating the OLR from different scene types; the mean value F_a is calculated from the contribution of the individual scenes by a proper weighting with the number of pixels belonging to a scene.

The inclusion of the WV channel information in the OLR retrieval is important since it more than halves the rms error in comparison with a single IR channel approach; the estimate of the absolute accuracy of the OLR retrieval technique was up to 20 W m^{-2} (Schmetz and Liu 1988), with the error being mainly systematic due to satellite calibration and errors inherent in the regression and in the preprocessed dataset. A discussion of systematic errors of the longwave cloud-radiative forcing is presented in the following section 3.

3. Bias error estimation

It is the aim of this section to quantify biases in the cloud-radiative forcing as retrieved from the METEOSAT radiances in the CDS. Four reasons, which could induce a bias in the retrieved mean flux F_a and especially in the clear sky flux F_{cl}, are discussed:

(a) calibration errors in the WV and IR channel of METEOSAT;

(b) a bias inherent in the regression algorithm;

(c) cloud contamination of clear sky radiance observations; and

(d) sampling of the clear sky upper tropospheric humidity field.

The net result of the bias estimation will also help explain CF_{lw} differences between this work and the study of Ramanathan et al. (1989).

a. Calibration error

Aboard geostationary spinning satellites like METEOSAT the large size of the aperture (about 40 cm) prevents an absolute onboard calibration of the complete radiometric system. For METEOSAT alternative vicarious methods based on radiative transfer calculations for the IR (Gaertner 1989) and WV channel (Schmetz 1989b) are used for calibration on a daily basis.

The present operational calibration method for the WV channel was introduced in September 1987; before that time the WV calibration coefficients were estimated by minimizing the difference between the upper tropospheric humidity derived from METEOSAT and radiosondes, respectively (Campbell 1982). The change to the method employing a radiative transfer model revealed that previous calibration coefficients were biased low by at least 5%. This bias in the calibration coefficient introduces an offset in the retrieved OLR that is absolutely larger for high outgoing fluxes exiting clear sky scenes, i.e., typically clear sky fluxes are underestimated by about 4–7 W m^{-2}, whereas the OLR from deep convective clouds with cold tops is underestimated by less than 1 W m^{-2}. A sensitivity test has shown that the use of the WV calibration coefficient provided in the official calibration reports (ESOC 1985) underestimates CF_{lw} by about 3–5 W m^{-2} in areas of the maximum forcing.

It has also been noted that the IR calibration coefficients were about 1.5%–2% too high (Koepke 1980; Asem et al. 1987). For the same reasoning as above this leads to a high bias error of about 2–3 W m^{-2} in the cloud forcing CF_{lw}. Thus, the estimated net bias of CF_{lw} due to calibration errors is an underestimation of the longwave cloud forcing by about 2–3 W m^{-2}.

b. Bias in the regression technique

The regression algorithm for estimating the OLR from IR and WV radiance observations (Eqs. 5 and 8) is based on least squares fits to radiative transfer calculations. As pointed out by SL (1988) the radiative transfer model tends to underestimate the clear sky OLR by about 4–6 W m^{-2} in comparison to line-by-line results. The absolute value of that bias decreases with the magnitude of the OLR, which obviously leads to a low bias error in the cloud-radiative forcing. Schmetz and Liu (1988) have also shown (see their Fig. 1) that the regression algorithm slightly underes-

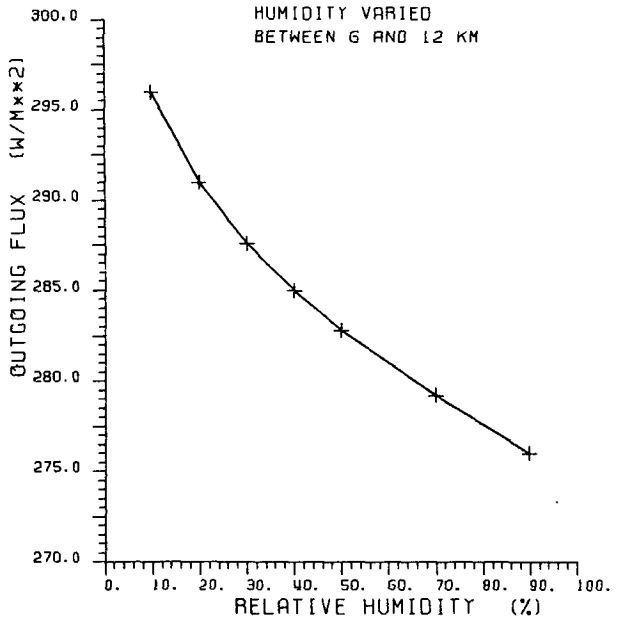

FIG. 1. Clear-sky outgoing longwave radiative flux as a function of the relative humidity of the upper troposphere between 6 and 12 km altitude.

timates high OLR values at satellite zenith angles larger than 40°, while the opposite is observed for low OLR values (note that this work presents results within the are of about 45°S to 45°N and 45°W to 45°E). The inherent bias in the regression technique underestimates the radiative forcing CF_{lw} by more than 5 W m^{-2} in cases of strong instantaneous $CF_{lw} > 150$ W m^{-2}; however, only a fraction (<2 W m^{-2}) of this instantaneous maximum bias will propagate to monthly means.

c. *Cloud contamination of clear sky radiances*

A difficulty in satellite retrievals of parameters representing the earth's surface is the contamination of the clear sky radiances by subpixel clouds (e.g., Saunders 1986). The multispectral histogram analysis used for the operational production of the CDS is also subject to such errors; i.e. it tends to underestimate radiances from clear sky scenes. It is evident from Eq. 1 that the cloud contamination problem leads to an underestimation of the cloud forcing CF_{lw}.

Recently Gaertner (1989) has analyzed the dependence of clear sky radiances over sea on cloud fraction; he observed a 1.5%–2% increase of clear sky IR radiances when reducing the cloud cover threshold from 80% to 10%. The change can be explained by the cloud contamination of clear sky scenes that decreases with cloud fraction. The equivalent underestimation of the clear sky flux is of the order 3–5 W m^{-2}, which we assume as the bias introduced in the clear sky OLR over areas with large cloud amounts.

d. *Sampling the upper tropospheric humidity field*

A bias in the clear sky OLR can be introduced by a conditional sampling of the clear sky upper tropospheric humidity field. The sampling is inherently conditional because humidity and clouds are correlated and a retrieval of clear sky radiances tries to minimize cloud contamination.

It is argued that a dry bias in the clear sky upper tropospheric humidity field increases with the footprint of radiometer if one carefully tries to avoid cloud contamination; this is plausible considering the correlation between cloud and humidity. The CDS used in this study is based on the analysis of high resolution METEOSAT image data with scanner footprints (pixels) of 5 km × 5 km at nadir; note also that the multispectral histogram analysis extracts clear sky radiances from cloud-free holes in segment regions of 32 × 32 pixels.

From recent work we can estimate how large a bias is introduced in the upper tropospheric humidity by avoiding segment areas where clouds occur; Turpeinen and Schmetz (1989) show that an upper tropospheric humidity of about 60% is a good threshold above which clouds at higher altitudes tend to occur on a segment scale, which is, on average, about 200 km × 200 km. Recently we have also studied monthly climatologies of clear sky upper tropospheric humidities derived from METEOSAT with the method described by Schmetz and Turpeinen (1988). We considered a segment as cloud-free if there was no cloud above 700 hPa; interestingly, we then found monthly mean upper tropospheric relative humidities of only 30%–40% in the ITCZ.

Figure 1 now shows the dependence of the clear sky OLR on the relative humidity between 6 and 12 km in a tropical standard atmosphere as computed with a radiative transfer model. It is observed that the clear sky OLR is less than 280 W m^{-2} for humid conditions (>60%) where clouds occur while it is about 286 W m^{-2} for a relative humidity of 30%–40%.

From the preceding discussion one may expect that clear sky radiance retrievals, which are confined to cloud free areas as large as about 200 km, could overestimate the clear sky OLR by about 3–5 W m^{-2} in comparison with the clear sky scenes in the CDS that are retrieved from cloud free areas of a scale of about 50 km.

The above arguments should be considered in the following presentation of results where we refer to results of Ramanathan et al. (1989) from ERBE (Earth Radiation Budget Experiment) for comparison. The footprint of the ERBE data is about 35 km at nadir and Ramanathan et al. were careful in selecting only scenes for which the eight surrounding pixels were also could-free. Therefore, we suggest that the clear sky fluxes from ERBE and the CDS, respectively, should be offset due to the sampling of the upper tropospheric

humidity. We cannot quantify the bias precisely, however, a value of about 3–5 W m^{-2} in convective regions seems reasonable.

e. Summary

In a comparison between our results and those of Ramanathan et al. (1989), it is to be expected that our forcing values are about 10–15 W m^{-2} lower in areas with strong convection. About 10 W m^{-2} of the bias appear to be due to errors in the present method using the operational product CDS with the calibration coefficients provided to METEOSAT users in the official "Calibration Report" (ESOC 1985). We believe that the results of Ramanathan et al. (1989) may exhibit a high bias of 3–5 W m^{-2} in convective regions due to a dry bias in the sampling of the upper tropospheric humidity field.

Since it is the primary purpose of this note to discuss the feasibility of retrieving the longwave cloud-radiative forcing from the METEOSAT CDS and to illustrate pertaining caveats, the results in the following section are not corrected for the different biases discussed above. In a future analysis one could consider the present study and make an attempt to correct for biases.

4. Results

a. Mean OLR

Figure 2 shows the monthly mean OLR for April 1985 for the center part of the METEOSAT field of view (45°S–45°N, 45°E–45°W). Largest OLR values exceeding 300 W m^{-2} are observed over the Sahara with two maxima over northern Chad and northern Sudan. Relatively high fluxes (>280 W m^{-2}) are also obtained over the Southern Hemisphere in an extended belt reaching from the central South Atlantic all across Africa. A comparison with Fig. 3 reveals that both areas of maximum OLR coincide with regions of minimum longwave cloud-radiative forcing; those clear regions are associated with the downward Hadley circulation.

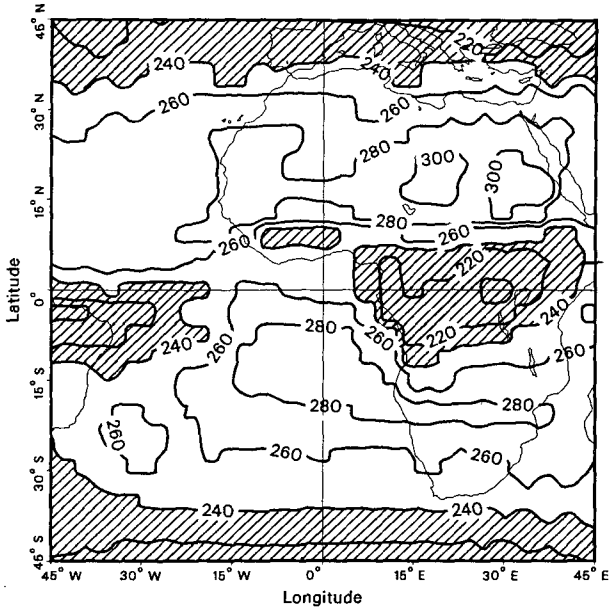

FIG. 2. Monthly mean outgoing longwave radiative flux (OLR) for April 1985. Regions with OLR values less than 240 W m^{-2} are hatched.

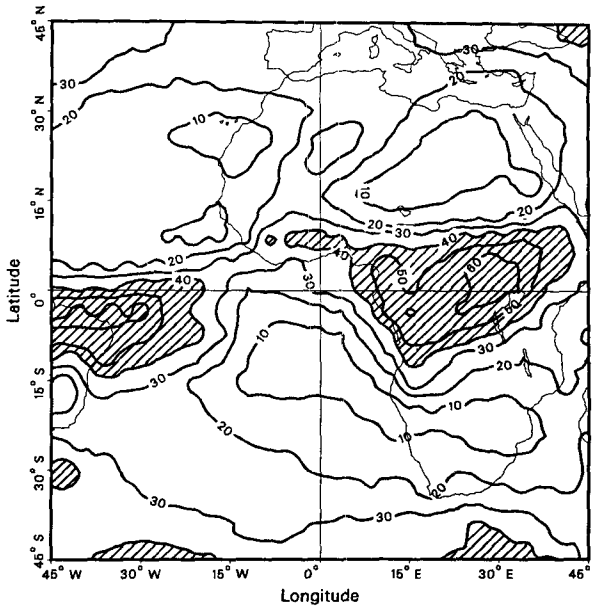

FIG. 3. Total longwave cloud-radiative forcing CF_{lw} for April 1985. Regions with CF_{lw} larger than 40 W m^{-2} are hatched.

The ITCZ shows two regions with values less than 220 W m^{-2}, a broad area over central Africa reaching from Ethiopia to the Atlantic coast of Cameroon and Gabon and a band along 5°S over Brazil and the adjacent Atlantic Ocean. The absolute minimum of 195 W m^{-2} is observed over the equator west of Lake Victora, this minimum being associated with the maximum CF_{lw} of about 70 W m^{-2}. OLR values less than 220 W m^{-2} around 45°N and 45°S are associated with the midlatitude disturbances.

b. Total longwave cloud-radiative forcing

Figure 3 shows the total longwave cloud-radiative forcing CF_{lw} (see Eq. 1). Values of CF_{lw} larger than 60 W m^{-2} are found in the continental ITCZ over Africa in two regions; first, an extended area situated in the equatorial region over Northeast Zaire, Uganda, and southern Sudan where values of nearly 70 W m^{-2} are observed. The strong forcing appears to be related to orographically enhanced convective activity; the spread of the area of high forcing in northeasterly direction seems related to high level could debris advected by the mean flow (e.g., Desbois et al. 1989). Secondly,

a small patch with $CF_{lw} > 60$ W m^{-2} is found over the Congo area, presumably reflecting the enhancement of the convective activity due to low level convergence, a conclusion that can be drawn from a monthly mean 850 hPa–wind analysis (ECMWF 1987). Another area with high forcing up to 65 W m^{-2} is observed over Brazil and the adjacent Atlantic Ocean. Small forcings of $CF_{lw} < 10$ W m^{-2} are found in the subtropical belts indicating the descending branch of the Hadley cell. The zonal belts of minimum cloud forcing over northern Africa is split by a band with a maximum $CF_{lw} = 35$ W m^{-2}, the band being due to high level cirrus of the subtropical jet stream that was well developed during the last ten days of April 1985.

A comparison with results for April 1985 from Ramanathan et al. (1989) shows excellent agreement of the geographical distribution of the longwave cloud-radiative forcing; also detailed features, like the minimum forcing over Brazil at 16°S, 45°W and the relative maximum at 30°S, 45°W, are found in both studies. The agreement confirms that condensed METEOSAT observations in the CDS are well suited for a relative monitoring of the longwave cloud-radiative forcing; as discussed above special care must be taken to identify potential sources for a bias.

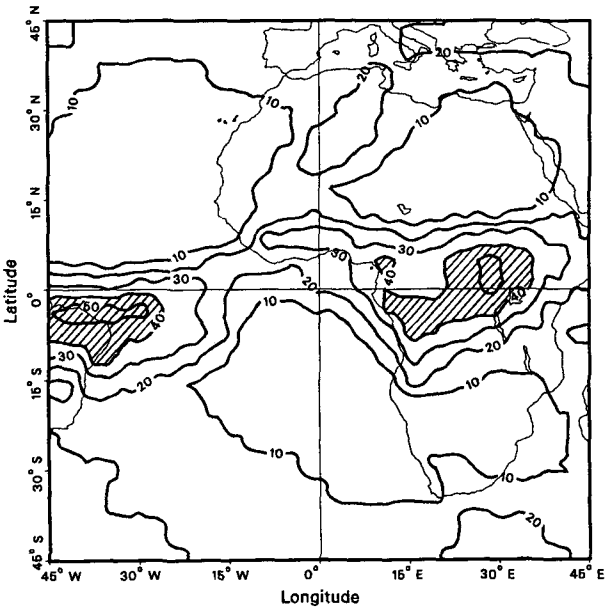

FIG. 4. Longwave cloud-radiative forcing due to high level clouds with tops ≤ 400 hPa. Regions with $CF_{lw,high}$ larger than 40 W m^{-2} are hatched.

c. *Contribution of different cloud levels*

Individual contributions of different cloud layers to the total cloud forcing may be obtained with Eq. 3 since the fractional cloud cover is provided for three levels of clouds in the CDS. Although the estimation of $CF_{lw,i}$ from different cloud layers i necessitates the use of fractional cloud amounts, which may have uncertainties of 10%–15%, it is considered a useful step towards estimating the vertical distribution of the cloud-radiative forcing. Previous workers (Slingo and Slingo 1988; Ramanathan et al. 1989) pointed out the importance of vertical profiles of cloud-radiative heating or the diabatic heating in general; in fact, the same value of CF_{lw} at the top of the atmosphere may be produced by very different profiles of local radiative heating/cooling. Therefore the vertical stratification of cloud forcing appears useful for validating general circulation models since it decreases the potential for compensating errors that could bring about a fallacious agreement between model results and observations. A coarse estimation of the vertical distribution of cloud induced radiative cooling/heating could even be obtained from the present dataset if additional information on cloud base was available.

1) HIGH LEVEL CLOUD

Figure 4 shows the cloud forcing $CF_{lw,high}$ solely due to clouds at altitudes higher than 400 hPa; the figure closely resembles the picture of the total cloud forcing in Fig. 3 indicating that high level clouds provide the major contribution to the total forcing CF_{lw}. A quantitative examination of the convectively active areas in the ITCZ reveals that 70%–80% of the total forcing is due to high clouds. No contribution of high cloud to CF_{lw} is observed over large areas in the subtropics, the jet area over the Sahara being an exception.

The observed values of high level CF_{lw} illustrate that the divergence of longwave radiation is an important diabatic heat source; even if the maximum values of high level forcing of about 50 W m^{-2} were spread throughout a layer of 300 hPa the mean diabatic heating would be about 1.5 K d^{-1} which is not at all negligible compared with the latent heat release (e.g., Ramanathan 1987). Sensitivity tests with a three-dimensional mesoscale model including moist convective processes and radiation have indicated that the longwave forcing mainly occurs in a shallow layer at cloud top enhancing destabilization of the upper cloud layer and speeding up convective development (Beniston and Schmetz 1985).

2) MEDIUM LEVEL CLOUD

Figure 5 depicts the forcing due to medium level cloud (700 ≥ cloud top > 400 hPa); areas with $CF_{lw,medium} > 10$ W m^{-2} are hatched. The maximum of 17 W m^{-2} is observed over the Ethiopian highland, corresponding to a relative contribution of some 35% of $CF_{lw,medium}$ to the total forcing. The importance of medium level clouds in the Ethiopian region has also been noted by Desbois et al. (1988) for July 1983; they found relatively low monthly mean IR brightness temperatures although very cold cloud occurred infre-

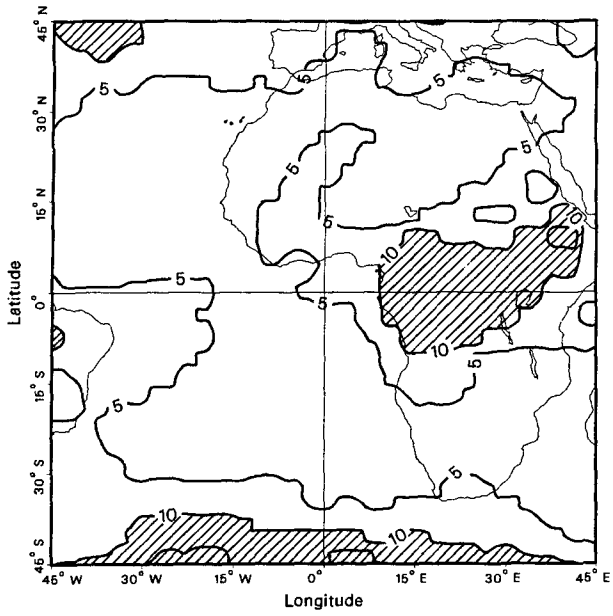

FIG. 5. As Fig. 4 except for longwave cloud-radiative forcing due to medium level clouds (700 hPa ≥ cloud top > 400 hPa). Regions with $CF_{lw,\text{medium}}$ larger than than 10 W m^{-2} are hatched.

quently, which indicates a frequent presence of medium level clouds.

Generally the relative contribution of medium level clouds to the total forcing is about 20% in the ITCZ. In the midlatitude westerlies of the Southern Hemisphere medium level clouds contribute more than one-third to the total forcing.

3) LOW LEVEL CLOUD

The value of $CF_{lw,\text{low}}$ (Fig. 6) exceeds 5 W m^{-2} over the extended marine regions covered with stratiform clouds and within the midlatitude westerlies, and the absolute maximum is about 10 W m^{-2} over the South Atlantic at 0° longitude and 18°S. An interesting feature is that the 5 W m^{-2} isoline appears parallel to the African west coast at a distance between 400 and 800 km. This could be explained by predominantly offshore winds and/or divergent winds at low levels during April 1985 as indicated by a 850 hPa wind analysis (ECMWF 1987). The existence of a virtually cloud-free band at low level bending along the West Africa coast was readily verified for most of the month by inspection of visible satellite images.

5. Conclusion

The purpose of this work was to examine the feasibility of estimating the longwave cloud-radiative forcing from the operationally produced METEOSAT Climatological Data Set (CDS). The CDS provides information on the IR and WV radiances from clear sky and cloudy scenes, thus enabling the direct calculation of the cloud forcing. A novel feature of the present work is the stratification of the longwave cloud-radiative forcing into three cloud level classes. This is useful for validating general circulation models since it decreases the potential for compensating errors; it can also provide a first estimate of cloud induced longwave radiative heating in the troposphere, which has been shown to influence the general circulation (Stuhlmann and Smith 1988).

A comparison of the longwave forcing from the METEOSAT CDS with data from ERBE (Ramanathan et al. 1989) shows excellent agreement in the geographical distribution, although METEOSAT estimates are about 10–15 W m^{-2} ($\approx$15%) lower in regions of maximum forcing. Deficient operational calibration, cloud contamination of clear-sky radiances are the major reasons for differences during the period under study (April 1985). Since then the calibration has been improved and a better clear-sky radiance retrieval will become operational in the near future. We suggest that the ERBE clear sky fluxes are likely to possess a high bias of 3–5 W m^{-2} due to sampling of the upper tropospheric humidity field, thus slightly overestimating the longwave cloud-radiative forcing.

The CDS is produced since July 1983 in a consistent manner without major retrieval changes; thus it can serve the purpose of establishing a relative climatology of longwave cloud-radiative forcing. As METEOSAT observations of CF_{lw} are liable to systematic errors (see section 3), due to calibration and the retrieval of the broadband OLR from narrowband radiances, one has to be cautious when using the data in quantitative cli-

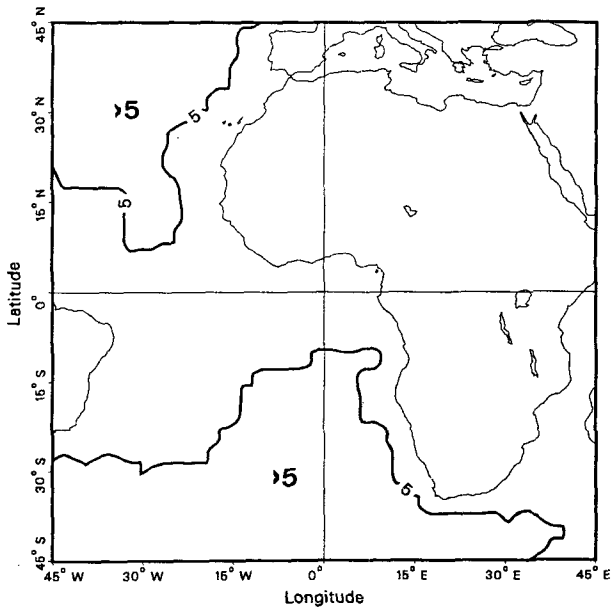

FIG. 6. As Fig. 4 except for longwave cloud-radiative forcing due to low level clouds (cloud top > 700 hPa).

mate studies. However, the observations ought to be useful for studying regional features of the cloud-radiative forcing CF_{lw} and for monitoring interannual variability in a qualitative manner (Ramanathan 1987).

Obviously one would wish to estimate the net effect of clouds on the radiation field, this requiring an extension of the flux retrieval to the solar METEOSAT channel. While the feasibility has already been demonstrated (Gube 1982), one can expect that the quality of the shortwave fluxes at the top of the atmosphere from METEOSAT will be compromised mainly by uncertain anisotropy and spectral corrections (Stuhlmann and Raschke 1987). Nevertheless the guaranteed continuity of observations from operational meteorological satellites qualifies those radiation observations as a useful complement to dedicated scientific experiments like ERBE. The usefulness may be enhanced with the advent of a new generation of geostationary satellites with better calibration and more imaging channels, the latter potentially reducing the uncertainty of narrowband-to-broadband conversions.

Acknowledgments. The authors appreciate suggestions on the manuscript by Mr. B. Mason. Thanks are due to the European Space Agency for providing a fellowship to Dr. M. Mhita.

REFERENCES

Abel, P. G., and A. Gruber, 1979: An improved model for the calculation of longwave fluxes at 11 μm, NOAA Tech. Rep., NESS 106, 24 pp.

Asem, A., P. Y. Deschamps and D. Ho, 1987: Calibration of the Meteosat infrared radiometer using split window channels of NOAA AVHRR. *J. Atmos. Oceanic Technol.*, **4**, 553–562.

Beniston, M., and J. Schmetz, 1985: A three-dimensional study of mesoscale model response to radiative forcing. *Bound.-Layer Meteor.*, **31**, 149–175.

Barkstrom, B. R., and G. L. Smith, 1986: The earth radiation budget experiment: Science and implementation. *Rev. Geophys.*, **24**, 379–390.

Bowen, R., and R. Saunders, 1984: The semitransparency correction as applied operationally to Meteosat infrared data. *ESA Journal*, **8**, 125–131.

Campbell, S. 1982: Vicarious calibration of METEOSAT's infrared sensors. *ESA Journal*, **6**, 151–162.

Cess, R. D., and G. L. Potter, 1987: Exploratory studies of cloud radiative forcing with a general circulation model. *Tellus*, **39A**, 460–473.

Coakley, J. A., and D. G. Baldwin, 1984: Towards the objective analysis of clouds from satellite imagery data. *J. Climate Appl. Meteor.*, **23**, 1065–1099.

Charlock, T. P., and V. Ramanathan, 1985: The albedo field and cloud radiative forcing produced by a general circulation model with internally generated cloud optics, *J. Atmos. Sci.*, **42**, 1408–1429.

Desbois, M., T. Kayiranga and B. Gnamien, 1989: Diurnal cycle of convective cloudiness over tropical Africa observed from Meteosat: Geographic characterization and interannual variation. *Ann. Geofis.*, **7**, 395–404.

——, ——, ——, S. Guessous and L. Picon, 1988: Characterization of some elements of the Sahelian climate and their interannual variations for July 1983, 1984 and 1985 from the analysis of METEOSAT ISCCP data. *J. Climate*, **1**, 867–904.

ECMWF, 1987: Daily global analysis. Operational data assimilation system: April–June 1985. ECMWF Reading, UK.

ESOC, 1985: METEOSAT-2 Calibration report, Issue 12, April–June 1985. [Available from: European Space Operations Centre/MEP, 6100 Darmstadt, FR Germany.]

Gaertner, V., 1989: MIEC IR calibration coefficients derived from cloud free sea pixels. *Proc. of the Seventh METEOSAT Scientific Users' Meeting*, Madrid, Eumetsat, EUM P 04, 15–18.

Gruber, A., and L. L. Stowe, 1989: An analysis of cloud radiation forcing as calculated from ERBE, AVHRR and Nimbus-7 ERB and cloud data. *Adv. Space Res.*, **9**(7), 129–138.

Gube, M., 1982: Radiation budget parameters at the top of the Earth's atmosphere derived from Meteosat data. *J. Appl. Meteor.*, **21**, 1907–1921.

Harrison, E. F., D. R. Brooks, P. Minnis, B. A. Wielicki, W. F. Staylor, G. G. Gibson, D. F. Young, F. M. Denn and the ERBE Science Team, 1988: First estimates of the diurnal variation of longwave radiation from the multiple-satellite earth radiation budget experiment (ERBE). *Bull. Amer. Meteor. Soc.*, **69**, 144–1151.

Hartmann, D. L., V. Ramanathan, A. Berroir and G. E. Hunt, 1986: Earth radiation budget data and climate research. *Rev. Geophys.*, **24**, 439–468.

Jones, M., and J. Morgan, 1981: Adjustment of the METEOSAT-1 radiometer response by ground processing. *ESA Journal*, **5**, 305–320.

Koepke, P., 1980: Calibration of the METEOSAT IR channel by ground measurements. *Beitr. Phys. Atmos.*, **53**, 442–444.

MEP (METEOSAT Exploitation Project), 1987: MIEC Processing, ESA STR-224, 21 pp.

Ramanathan, V., 1987: The role of earth radiation budget studies in climate and general circulation research. *J. Geophys. Res.*, **92**(D4), 4075–4095.

——, R. D. Cess, E. F. Harrison, P. Minnis, B. R. Barkstrom, E. Ahmad and D. Hartmann, 1989: Cloud-radiative forcing and climate: Results from the Earth Radiation Budget Experiment. *Science*, **243**, 57–63.

Saunders, R. W., 1986: An automated scheme for the removal of cloud contamination from AVHRR radiances over western Europe. *Int. J. Remote Sens.*, **7**, 867–886.

Schmetz, J. 1989a: Cloud observations from METEOSAT and the inference of winds. *Adv. Space Res.*, **9**(7), 91–99.

——, 1989b: Operational calibration of the Meteosat water vapor channel by calculated radiances. *Appl. Opt.*, **28**, 3030–3038.

——, and Q. Liu, 1988 (SL, 1988): Outgoing longwave radiation and its diurnal variation at regional scales derived from METEOSAT, *J. Geophys. Res.*, **93**(D9), 11192–11204.

——, and O. M. Turpeinen, 1988: Estimation of the upper tropospheric relative humidity field from METEOSAT water vapor image data. *J. Appl. Meteor.*, **27**, 889–899.

Schneider, S. H., 1972: Cloudiness as a global feedback mechanism: Effects on the radiation balance and surface temperature of variations in cloudiness. *J. Atmos. Sci.*, **29**, 1413–1422.

Slingo, A., and J. M. Slingo, 1988: The response of a general circulation model to longwave cloud radiative forcing. I: Introduction and initial experiments. *Quart. J. Roy. Meteor. Soc.*, **114**, 1027–1062.

Stuhlmann, R., and E. Raschke, 1987: Satellite measurements of the earth radiation budget: Sampling and retrieval of sortwave exitances—a sampling study. *Beitr. Phys. Atmos.*, **60**, 393–410.

——, and G. L. Smith, 1988: A study of cloud-generated heating and its generation of available potential energy. Part II: Results for a climatological zonal mean January. *J. Atmos. Sci.*, **45**, 3928–3943.

Turpeinen, O., and J. Schmetz, 1989: Validation of the upper tropospheric relative humidity determined from METEOSAT data. *J. Atmos. Oceanic Technol.*, **6**, 359–364.